




# Dependence of the magnetoelectric coupling on elastic and dielectric properties of two-phase multiferroic composites

M. Naveed-Ul-Haq<sup>1,\*</sup> , Vladimir V. Shvartsman<sup>2</sup>, Vytautas Samulionis<sup>3</sup>, Maksim Ivanov<sup>3</sup>, Juras Banys<sup>3</sup>, and Doru C. Lupascu<sup>2</sup>

<sup>1</sup>Department of Physics, COMSATS University Islamabad, Lahore Campus, 1.5 km Off Raiwind Road, Lahore 54000, Pakistan

<sup>2</sup>Institute for Materials Science and Center for Nanointegration Duisburg-Essen (CENIDE), University of Duisburg-Essen, Universitätsstrasse 15, 45141 Essen, Germany

<sup>3</sup>Faculty of Physics, Vilnius University, Saulėtekio al. 9/IIIb., 10222 Vilnius, Lithuania

Received: 22 March 2021

Accepted: 16 June 2021

Published online:  
24 June 2021

© The Author(s), under exclusive licence to Springer Science+Business Media, LLC, part of Springer Nature 2021

## ABSTRACT

We report on temperature-dependent studies of ultrasonic and dielectric properties of  $(x)0.5(\text{Ba}_{0.7}\text{Ca}_{0.3})\text{TiO}_3-0.5\text{Ba}(\text{Ti}_{0.8}\text{Zr}_{0.2})\text{O}_3(\text{BCZT})/(1-x)\text{NiFe}_2\text{O}_4$  (BCZT/NFO) composite multiferroics and their relationship to the magnetoelectric (ME) effect in these materials. The most decisive factor in the maximization of the ME effect is the strong elastic softening of the BCZT phase at the phase transition between its ferroelectric phases with orthorhombic and tetragonal symmetry. The proximity of this phase transition to room temperature makes the system promising for practical applications of the ME effect. The magnetostrictive phase does not play any direct role in the determination of the ME temperature dependence because of its weakly temperature-dependent mechanical properties.

## Introduction

Magnetoelectric multiferroics are a fascinating class of materials, in which not only magnetic and ferroelectric orders coexist, but also a cross-coupling occurs between magnetic and electric degrees of freedom. This cross-coupling, i.e., the magnetoelectric effect, allows the application of these materials for the development of weak magnetic field sensors,

low-power consuming magnetic-read/electric write memory elements, or energy harvesting devices [1–6].

There are two distinct groups of multiferroic materials: the single-phase and the multiphase (or composites). Single-phase multiferroics have certain inherent drawbacks preventing them from application. The foremost is the difficulty of the simultaneous existence of ferroelectricity and ferromagnetism in the same crystal phase [3]. The other being the

Handling Editor: David Cann.

Address correspondence to E-mail: naveedulhaq@cuilahore.edu.pk

appearance of multiferroicity as well as magneto-electric (ME) coupling at temperatures much lower than room temperature. On the contrary, composite multiferroics, where chemically different magnetic and ferroelectric phases are “artificially” connected, offer a convenient way to achieve sizable magneto-electric coupling at room temperature [3]. These two-phase magnetoelectrics can be fabricated with a variety of configurations, including particulate composites (with 3–3 or 3–0 connectivity) [4], pillar-matrix (1–3 connectivity) [5], and the layer-by-layer (2–2 connectivity) type [6].

There has been a great deal of theoretical as well as experimental research on composite multiferroics over the past two decades [7–10]. Several mechanisms of coupling between the magnetic and electric properties of the constituents have been exploited. The most popular mechanism is based on a mechanically mediated coupling between a piezoelectric and magnetostrictive material, i.e., an applied electric field generates stress at the interface due to the piezoelectric effect in one phase, which induces a change of the magnetization on the second phase due to the Villari effect (inverse magnetostriction). Thus, a variation of the magnetization under the action of an electric field, i.e., the converse magneto-electric effect, is achieved. Research is geared toward the synthesis of new multiferroics as well as finding new routes to enhance the ME coupling within them. When looking for new composite multiferroics, the proper choice of the ferroelectric/piezoelectric and the magnetostrictive material is very important. While it is natural that the mechanical properties of the composites are critical to achieving large magneto-electric coupling [5, 8, 9], they have not been studied as intensively as ferroelectric or magnetic characteristics of the composites.

Recently we have demonstrated the significant magneto-electric effect in bulk composite ceramics of  $(x)0.5(\text{Ba}_{0.7}\text{Ca}_{0.3})\text{TiO}_3-0.5\text{Ba}(\text{Ti}_{0.8}\text{Zr}_{0.2})\text{O}_3(\text{BCZT})/(1-x)\text{NiFe}_2\text{O}_4(\text{NFO})$  [10, 11]. In the present paper, we report on studies of the temperature dependence of the elastic properties of the composites using an ultrasonic technique. We compare the obtained data with the dielectric and magneto-electric properties and show that the maximal ME response occurs in the temperature range of the largest elastic compliance of the composites.

## Experimental

The ceramic samples of BCZT, NFO, and their composites were prepared by the conventional solid-state reaction. All composite ceramics were sintered at 1200 °C for 6 h, the pure BCZT was sintered at 1450 °C for 6 h, while the pure NFO was sintered at 1150 °C for 6 h. Further synthesis and characterization details about the composites can be found in our earlier publication [10]. The pulse-echo method at 10 MHz frequency was utilized to measure the ultrasonic velocity and attenuation in all samples [12]. For excitation and detection of longitudinal ultrasonic waves piezoelectric z-cut lithium niobate transducers were used. Apiezon grease was applied on polished parallel surfaces of the ceramic samples to make acoustic contacts. The typical thickness of samples along the direction of ultrasonic wave propagation was about 3–4 mm. The silver paste was painted onto both sides and electrical contacts were made using copper wire for dielectric measurements. The real and imaginary parts of the dielectric permittivity were measured with a Wayne Kerr 4275 LCR meter interfaced to a computer and controlled by a custom designed LabView software. For temperatures below 300 K, a cryostat from Janis Research (model CCS-350) attached to a Lakeshore 331 temperature controller was utilized. Above 300 K, a custom-built sample stage was used. The converse magneto-electric effect was measured using a modified commercial SQUID ac-susceptometer (Quantum Design, model 1822) [13].

## Results

To understand and compare the ultrasonic behavior in composites, it is necessary to study the ultrasonic behavior of the pure constituents of the composite at first. There are only a few papers on the elastic properties of pure BCZT ceramics reporting data measured at low frequencies [14–16]. Therefore, it has been of additional interest to measure the temperature dependence of the elastic properties at ultrasonic frequencies. Panels (a) and (b) of Fig. 1 show the temperature dependences of the ultrasonic velocity and attenuation measured on cooling in the 200–400 K temperature range in the pure BCZT ceramic. Several anomalies of the ultrasonic velocity and attenuation can be seen. The highest temperature

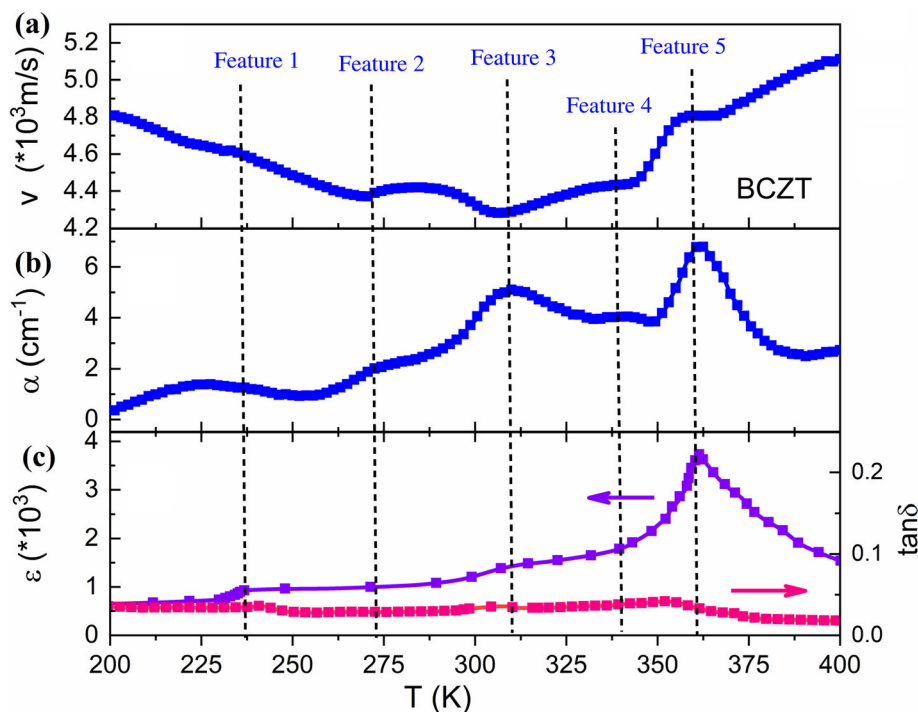
anomaly is around 360 K and corresponds to the paraelectric cubic (PE) to ferroelectric tetragonal ( $FE_T$ ) (T–C) phase transition (marked in Fig. 1 by Feature 5). Here, the critical slowing down of the ultrasonic velocity and the related attenuation peak appears. This T–C transition is also visible in the temperature dependences of dielectric permittivity and loss tangent of BCZT, which are shown in Fig. 1c. Upon further cooling, the ultrasonic velocity continues to decrease with a small anomaly at 340 K (corresponding to a small diffuse peak in attenuation marked as Feature 4). At 310 K there is a global minimum in the velocity and a peak of the attenuation (designated as Feature 3). Such elastic softening near the tetragonal to orthorhombic (O–T) phase boundary was observed in earlier low-frequency elastic studies [14–16]. This O–T transition is also detected in the permittivity data. The ultrasonic velocity begins to increase at lower temperatures, showing the elastic hardening of the BCZT piezoelectric material. A shallow minimum of the ultrasonic velocity and a shoulder-like anomaly in the attenuation near 270 K (Feature 2) can be related to the orthorhombic–rhombohedral (R–O) phase transition (undetected in the permittivity graph). All these three elastic anomalies have also been observed in literature for elastic compliance [13] and the elastic storage modulus [15]. Besides, we observed one

additional anomaly near 240 K (within the rhombohedral phase region, designated as Feature 1) which is detected in the velocity, attenuation, and permittivity plots. This anomaly (Feature 1) can be attributed to the interaction of the domain walls with defects, the coexistence of different ferroelectric phases, which is typical for the compositions close to the morphotropic phase boundary [15], or indicate a transition to another rhombohedral phase at 230 K [15].

The data for the acoustic wave velocity measured for a pure NFO sample are shown in Fig. 2. We observe a continuous hardening of the material on cooling and a small anomaly at about 310 K. This anomaly cannot be associated with a structural phase transition of NFO, therefore can be attributed to some internal stresses. Thus, comparing the temperature dependencies of the elastic properties of the constituents (BCZT and NFO), we can assume that any anomalous elastic behavior of the composites in the studied temperature range is associated with the acoustic response of the BCZT component only.

In panels (a) and (b) of Figs. 3, 4, 5, and 6 the temperature-dependent ultrasonic data for the BCZT80-NFO20, BCZT70-NFO30, BCZT60-NFO40, and BCZT50-NFO50 composite ceramics are displayed, while panel (c) in each case shows the dielectric properties. All samples show some

**Figure 1** **a** Ultrasonic velocity, **b** attenuation, and **c** the dielectric permittivity and tangent loss of the BCZT ceramic as a function of temperature. The vertical dashed lines show the anomalies common to all four properties.



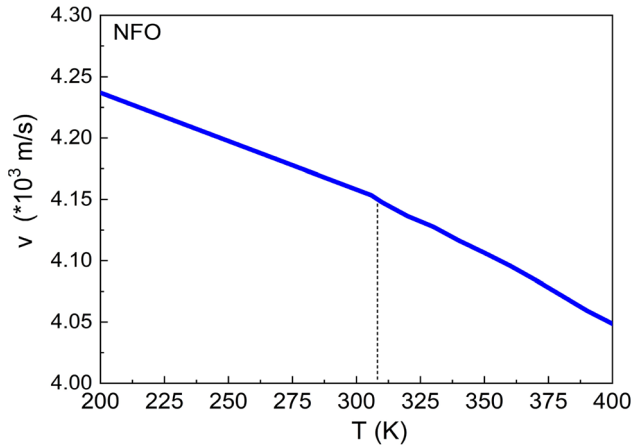
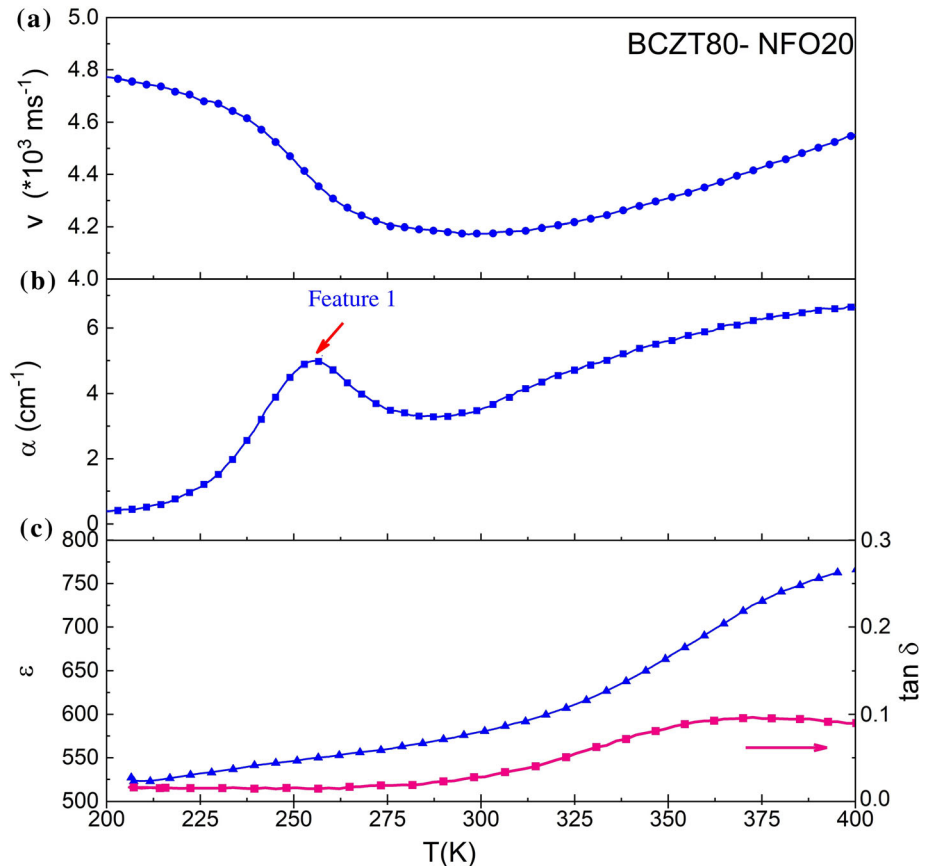


**Figure 2** Ultrasonic velocity of the NFO ceramics. There is a small anomaly at ~ 310 K; however, no structural phase transition can be associated with this.

interesting features: for BCZT80-NFO20 there is a broad maximum of the ultrasonic attenuation around 255 K (close to Feature 1 of BCZT), which corresponds to the rapidly decreasing ultrasonic velocity. The attenuation shows a monotonic increase after 290 K. In comparison to pure BCZT, The anomalies

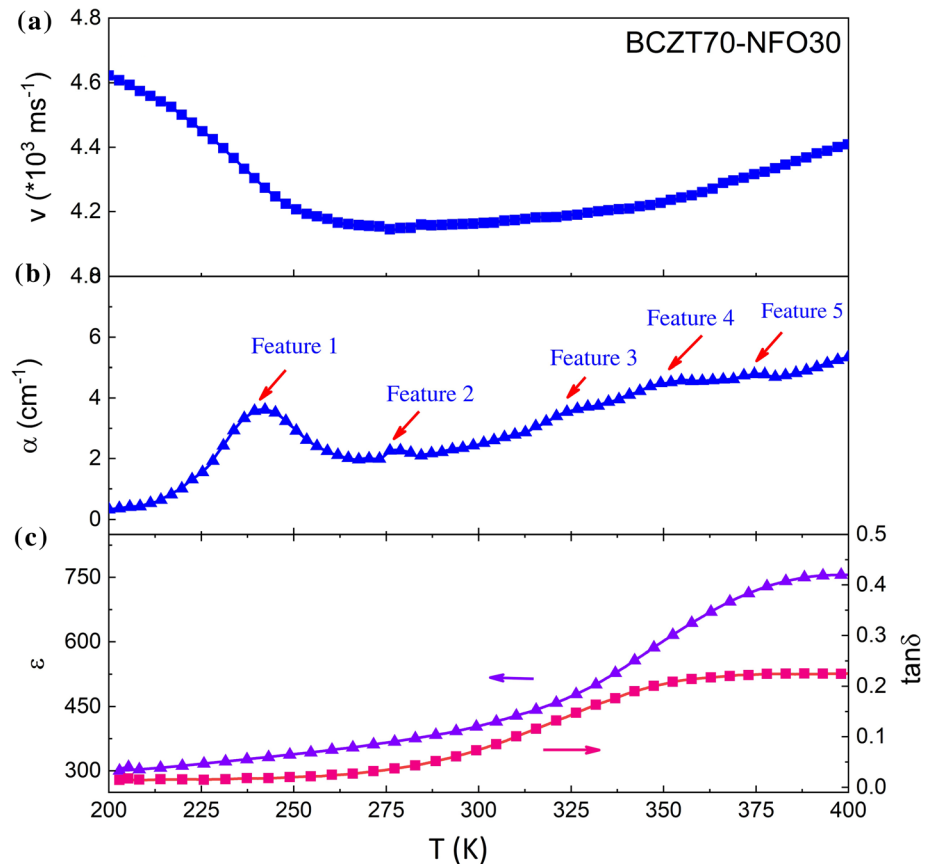
**Figure 3 a** Ultrasonic velocity, **b** attenuation, and **c** dielectric permittivity plus dielectric loss tangent of the BCZT80-NFO20 sample.



observed in the temperature dependence of the attenuation in the composite BCZT70-NFO30 to a good extent resemble those in the pure BCZT (Fig. 4). However, features 3, 4, and 5 are less pronounced and are shifted to higher temperatures: 324 K, 350 K, and 373 K, respectively, as compared to those of pure BCZT. In the case of BCZT60-NFO40, Feature 1 is reproduced which lies at 246 K (Fig. 5). Other than that, there are two other discernible features: one at 325 (Feature 3) and the other at 340 K (Feature 4). In the case of BCZT50-NFO50 (Fig. 6), Feature 1 is there but it is shifted to 258 K. Also, there is a broad feature in the temperature range between 310 and 350 K. All composite samples exhibit a wide minimum of the ultrasound velocity at 280–300 K, which becomes flatter in samples with less content of BCZT.

The features that we observed in pure BCZT are not reproduced in some composites, which can be due to the difference between the mechanical nature of BCZT and the composites, namely a stiffening of the BCZT by the CFO. The mechanical properties of a ceramic sample depend upon its microstructure. In the case of ferroelectric ceramics in general, e.g., in

**Figure 4** **a** Ultrasonic velocity, **b** attenuation, and **c** dielectric permittivity plus dielectric loss tangent of the BCZT70-NFO30 sample.

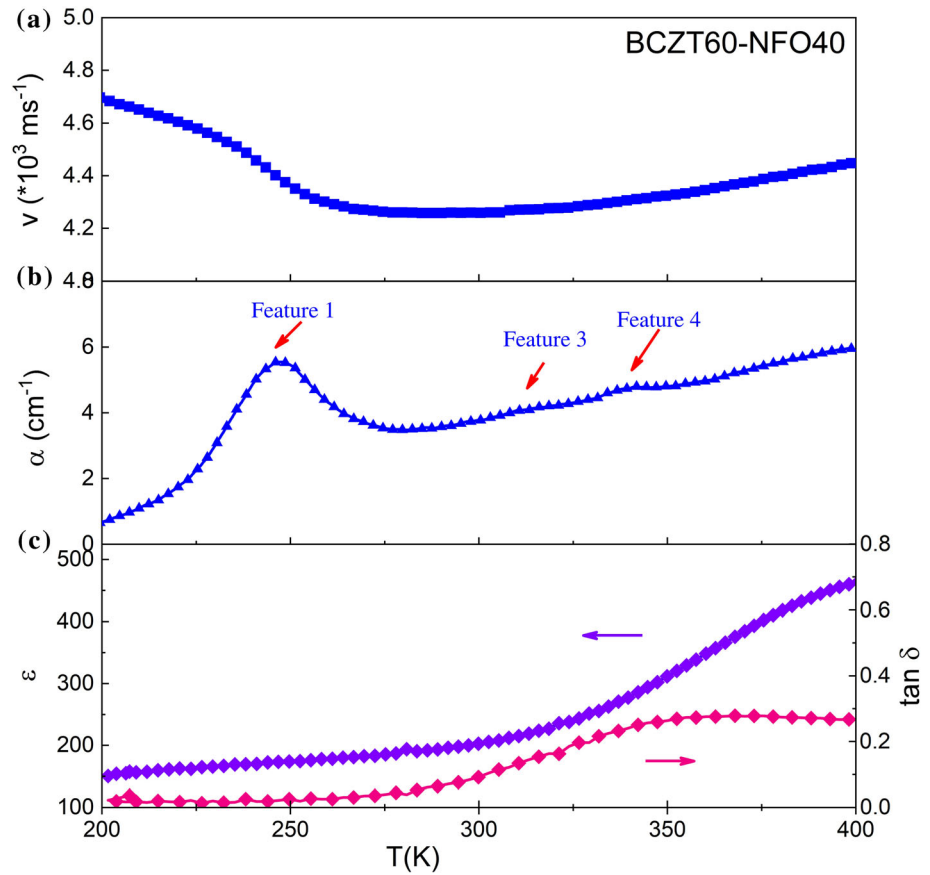


BCZT, there is a clear relationship between microstructure and elastic properties as has been studied by various researchers [17, 18]. An improvement in mechanical properties up to a critical grain size has been observed in these ceramics and the critical grain size varies according to the chemical composition as well as with the route of synthesis of powders and subsequent sintering [19]. In the case of BCZT, the critical grain size is about  $10 \mu\text{m}$  [20]. However, in the case of ferroelectric–ferromagnetic composites, the grain size does not remain homogeneous with an increase in ferrite content as can be seen in Fig. 7b–e. The overall elastic properties of the ceramics also depend upon a cumulative effect of grain size and porosity. The grain size combined with porosity determines the overall densification of the samples [21]. As we observe in Fig. 7, the porosity and grain size are not uniform in the composite samples, which might be the reason why the exact elastic features of pure BCZT are not efficiently reproduced in the composites.

### Temperature-dependent dielectric data

The panels (c) in Figs. 3, 4, 5 and 6 show the temperature dependence of the real part and loss tangent of dielectric permittivity of the BCZT-NFO composites measured at 10 kHz. The samples with the lower NFO content display a broad maximum of the dielectric permittivity above 350 K, which may be attributed to the Curie temperature of the ferroelectric component BCZT (as depicted clearly for pure BCZT in Fig. 1c). In the composites with the larger NFO content (40% and more) no maximum, but a “shoulder,” is observed and the dielectric permittivity grows continuously on heating (Figs. 5c and 6c). In all composites, the value of the dielectric permittivity strongly increases for decreasing frequency. Such behavior is related to the increasing conductivity contribution, which becomes significant in the composites with a large amount of the NFO (due to its semiconducting nature) in the insulating BCZT matrix; thus, the ferrite grains provide an easy conduction path across the sample thickness. Even in the composite with 20% of NFO, the maximum dielectric permittivity is smaller and significantly broader than

**Figure 5** **a** Ultrasonic velocity, **b** attenuation, and **c** dielectric permittivity plus dielectric loss tangent of the BCZT60-NFO40 sample.



in pure BCZT. This kind of dielectric behavior has already been reported in similar two-phase multi-ferroic composites [22–24]. The dielectric loss tangent shows a consistent behavior in all samples, it starts to increase around 270 K and its values saturate above 350 K. The other important point to be noted is that the value of the loss tangent increases almost linearly with the increasing NFO content, thereby confirming the detrimental role played by the ferrite content in terms of the overall dielectric permittivity of the composite, namely the conductive contribution to the dielectric permittivity.

**Temperature-dependent magnetoelectric coupling**

Figure 8 shows the temperature-dependent values of the varying magnetic moment induced by an *ac* electric field of  $E_{ac} = 200$  V/mm, also known as the converse magnetoelectric effect. These data were published and are discussed in Ref. [10]. To maximize the magnetoelectric response, a magnetic dc bias field was applied [10]. For all samples, the

magnetoelectric effect shows a broad maximum, the position of which depends on the composition. So, for the composite with 20% of NFO, the maximum of the ME effect is observed at 270 K and it shifts toward 330 K in the composite with 50% of NFO.

**Discussion**

The ultrasonic velocity,  $v$ , and attenuation,  $\alpha$ , are related to the real and the imaginary parts of the elastic modulus via equation [25]:

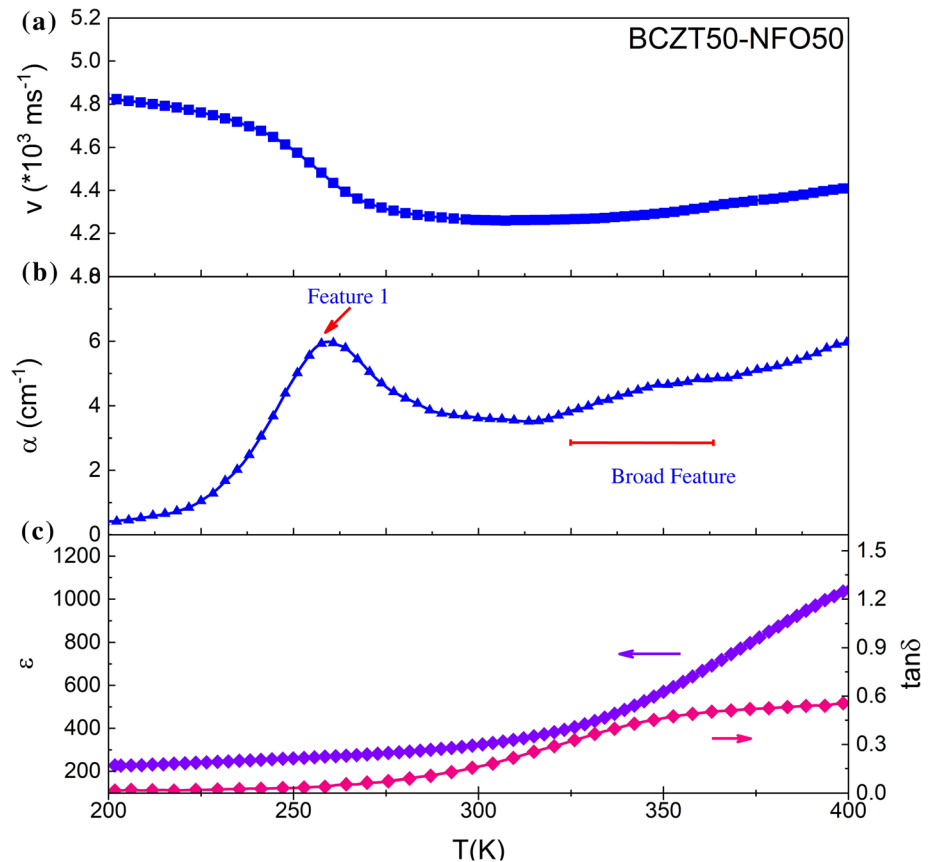
$$\frac{1}{v} - i \frac{\alpha}{\omega} = \sqrt{\frac{\rho}{\text{Re}(c) + i\text{Im}(c)}} \tag{1}$$

In the limit of the low attenuation, the approximate relationships are obtained as followed:

$$v = \sqrt{\frac{\text{Re}(c)}{\rho}} \tag{2}$$

$$\alpha = \frac{\omega}{2\rho v^3} \text{Im}(c) \tag{3}$$

**Figure 6** **a** Ultrasonic velocity, **b** attenuation, and **c** dielectric permittivity of BCZT50-NFO50 sample.



One can see that the ultrasonic attenuation and velocity have an inverse cubic relationship. Measuring the velocity and attenuation gives us information about the elastic modulus,  $c$ , or the compliance,  $s = c^{-1}$ , of the material, and effectively any anomaly in the temperature-dependent ultrasonic properties mimics the elastic response of the material.

Let's now establish a theoretical relationship between ultrasonic properties, electric permittivity, and the converse piezoelectric coupling and try to find whether there exists a meaningful correlation among them or not. The converse ME effect in mechanically coupled multiferroic composites is given by

$$M_{ME,ac} = c_{\text{eff}}^* \cdot q \cdot d \cdot E_{ac}, \quad (4)$$

where  $c_{\text{eff}}^*$  is the effective stiffness of the interface between two phases of the composite,  $d$  is the piezoelectric coefficient of the ferroelectric phase, and  $q$  is the effective piezomagnetic coefficient (the magnetic field derivative of magnetostriction) of the magnetic phase [9]. Strictly speaking, the coefficients in the formula are tensors of third and fourth rank, but for simplicity, we will not consider the tensor

form here. As we are considering a uniaxial loaded polycrystalline ceramic, the approximation is roughly valid on the averaged values and is typically applied in disk-shaped devices [21]. Since the elastic and magnetoelastic properties of the NFO phase do not show any significant anomaly in the studied temperature range (see Fig. 2) we can assume that the maximum of the ME effect is not due to the contribution of the magnetic phase. Therefore, we shall focus on the ultrasonic response of the ferroelectric phase and explore the relationship between the elastic properties of the BCZT phase and the ME properties of the composites. For this purpose, we need to go back to the elastic response of pure BCZT as depicted in Fig. 1.

There are several anomalies found in the attenuation data and some of them match the dielectric data of BCZT, the important ones are displayed in Fig. 1 as already discussed. These detected anomalies in pure BCZT samples are reproduced only partially in the acoustic and dielectric data of the composites. Now let's take a look at Fig. 8 where we notice that the broad maxima in the converse piezoelectric

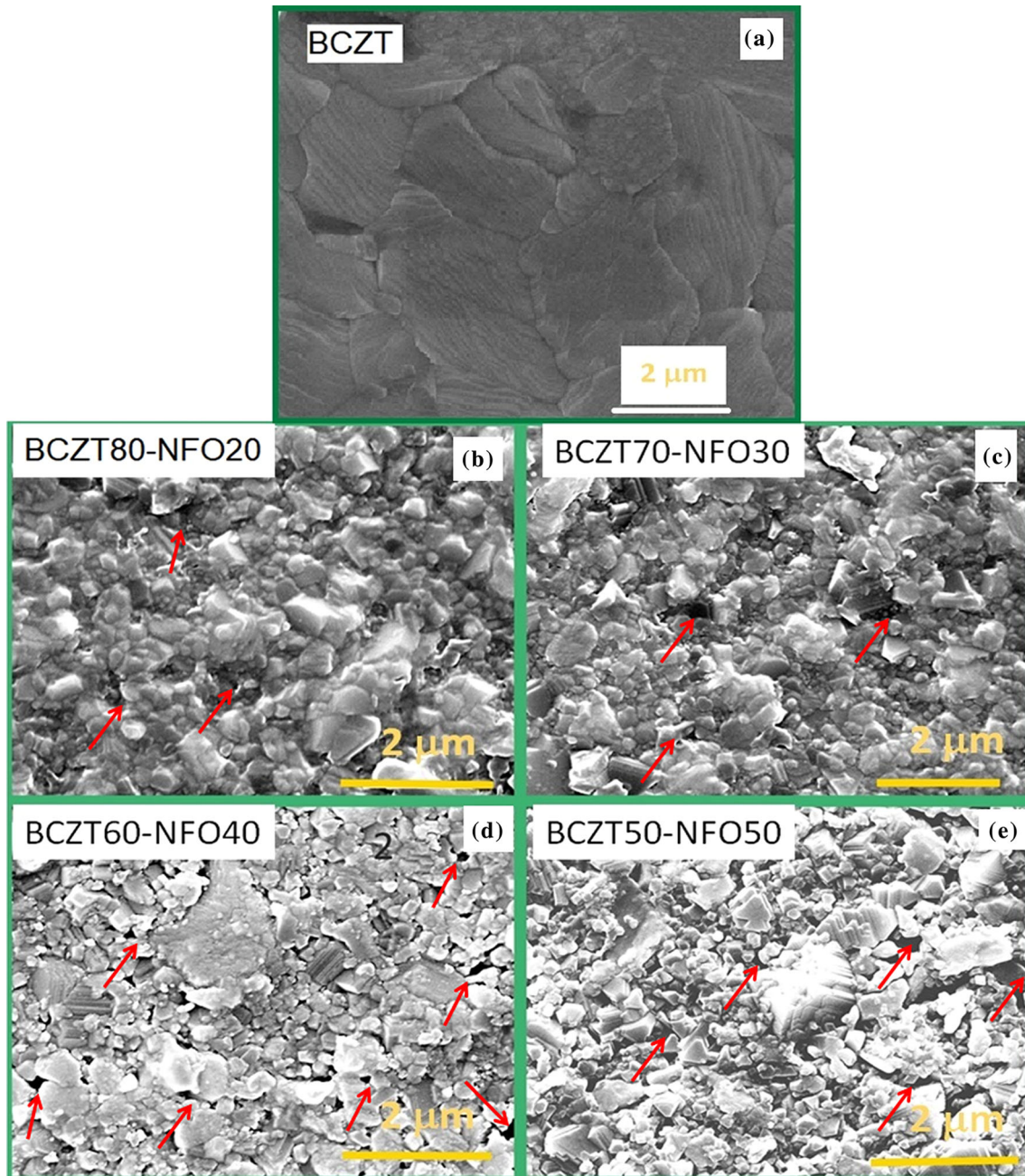


**Figure 7** SEM micrographs for all samples. The BCZT sample in **a** shows large grains and all grains are interfused. The composite samples in **b–e** show smaller grains and there are several pores/voids which are indicated by arrow symbols.

effect of the samples occur in the same temperature range where the Features 1–3 lie for the pure BCZT (the locations of these features are indicated by the dashed lines). The center of the maximum for the BCZT80-NFO20 sample lies near 275 K where Feature 2 (the R–O phase transition temperature) lies. On the other hand, the maxima of the ME curve for BCZT70-NFO30 and BCZT60-NFO40 are in the vicinity of Feature 3 (the O–T phase transition

temperature). For BCZT50-NFO50, the maximum is shifted to higher temperature, i.e., 335 K indicating an enhanced role of Feature 4 which lies at  $T_C$ . We could not verify the exact role of the transition at  $T_C$  to the ME coupling, since our ME data are limited up to 350 K. This overall behavior of the composites under study also matches with previous reports on the elastic properties of BCZT ceramics, in which the elastic softening is reported to be more pronounced



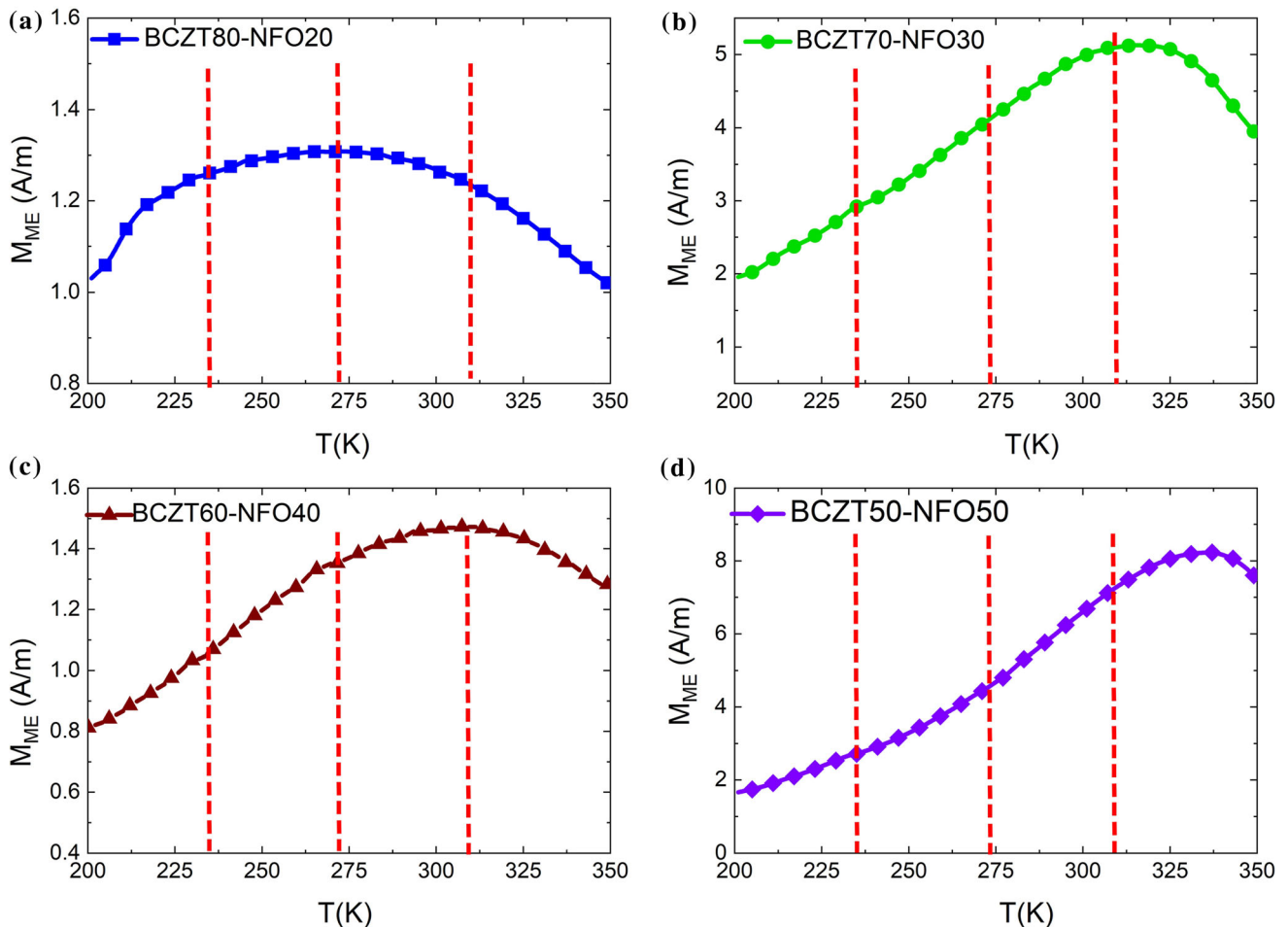


**Figure 8** Temperature-dependent converse ME effect for **a** BCZT80-NFO20, **b** BCZT70-NFO30, **c** BCZT60-NFO40, and **d** BCZT50-NFO50. These data for this image are reproduced from

Ref. [10] with permission from Elsevier/Acta Materialia. The dashed lines indicate the positions of the first three features from Fig. 1.

in the vicinity of the O–T phase boundary than that at the R–O, or in the O single-phase region [14]. This was rationalized by the divergence of the shear components of the elastic compliance at the O to T phase boundary [26–28]. Rotation of the spontaneous polarization from the [100] to the [110] direction is accompanied by an enhanced shear occurring in the  $yz$  or  $xz$  planes. It was also shown that this high softening together with the reduced anisotropy and large polarization is responsible for the maximized piezoelectric effect [15, 16, 28].

It is important to note here that according to the features displayed in the temperature-dependent ultrasonic velocity and attenuation, the temperature-dependent ME curves should have displayed peaks/maxima at or near Feature 1; however, this is not exactly the case. This can be explained, if we consider the values of frequency at which the

ultrasonic properties and the converse ME coupling are measured. The ultrasonic properties were measured at 10 MHz while the ME measurements were done at 8 Hz due to the available setup designs. It was found in earlier investigations of Damjanovic et al. [29] and Cordero et al. [14] that at low measurement frequencies, the temperature-dependent elastic anomalies merge into a single smeared maximum. Now considering Eq. (4) we can derive that the maximum of the magnetoelectric effect is related to the elastic and dielectric properties of the piezoelectric BCZT and we find these properties are maximized near the O–T phase transition.

## Conclusions

To get insight into the peculiarities of magnetoelectric coupling in the BCZT-NFO bulk multiferroic composites, we compared the temperature-dependent ultrasonic, dielectric, and magnetoelectric responses of these materials. We observed that the range of the maximal ME effect coincides with the anomalies in ultrasonic properties. Thereby the most significant factor determining the value of the ME coupling in the studied composites is the increase in the elastic compliance at the polymorphic orthorhombic–tetragonal phase transition, resulting in a significant growth of the piezoelectric coefficient. The proximity of this transition to room temperature makes the effect very promising for applications. Moreover, it was argued that the highest value of the elastic compliance along the O–T phase boundary is a general feature of BaTiO<sub>3</sub>-based compounds. It opens a good opportunity to optimize the room temperature value of the ME coupling of two-phase mechanically coupled multiferroic composites by choosing the ferroelectric constituent. The possible effect of structural phase transitions of the magnetic counterpart on its elastic properties and related ME effect is an interesting topic and can be a subject of future studies.

## Acknowledgements

Even though dating back several years now, this work would not have been possible without the financial support by the Deutsche Forschungsgemeinschaft (DFG, project Lu729/12) in the framework of the core program FOR 1509 “Ferroic Functional Materials – Multiscale Modelling and Experimental Characterization.”

## Data availability

The data reported in this manuscript are available from the corresponding author on a reasonable request.

## Declarations

**Conflicts of Interest** The authors declare that they have no conflict of interest.

## References

- [1] Nan CW, Bichurin MI, Dong S, Viehland D, Srinivasan G (2008) Multiferroic magnetoelectric composites: Historical perspective, status, and future directions. *J Appl Phys* 103(3)
- [2] Viehland D, Wuttig M, McCord J, Quandt E (2018) Magnetoelectric magnetic field sensors. *MRS Bull* 43(11):834–840
- [3] Hill NA (2000) Why are there so few magnetic ferroelectrics? *J Phys Chem B* 104(29):6694–6709
- [4] Etier M, Schmitz-Antoniak C, Salamon S, Trivedi H, Gao Y, Nazrabi A, Landers J, Gautam D, Winterer M, Schmitz D, Wende H, Shvartsman VV, Lupascu DC (2015) Magnetoelectric coupling on multiferroic cobalt ferrite-barium titanate ceramic composites with different connectivity schemes. *Acta Mater* 90:1–9
- [5] Schmitz-Antoniak C, Schmitz D, Borisov P, De Groot FMF, Stienen S, Warland A, Krumme B, Feyerherm R, Dudzik E, Kleemann W, Wende H (2013) Electric in-plane polarization in multiferroic CoFe<sub>2</sub>O<sub>4</sub>/BaTiO<sub>3</sub> nanocomposite tuned by magnetic fields. *Nat Commun* 4(1):1–8
- [6] Naveed-UI-Haq M, Webers S, Trivedi H, Salamon S, Wende H, Usman M, Mumtaz A, Shvartsman VV, Lupascu DC (2018) Effect of substrate orientation on local magnetoelectric coupling in bi-layered multiferroic thin films. *Nanoscale* 10(44):20618–20627
- [7] Cao Y, Wu B, Zhu YL, Wang YJ, Tang YL, Liu N, Liu JQ, Ma XL (2021) Self-assembled three-dimensional framework of PbTiO<sub>3</sub>:ε-Fe<sub>2</sub>O<sub>3</sub> nanostructures with room temperature multiferroism. *Appl Surf Sci* 544:148945
- [8] Palneedi H, Annapureddy V, Priya S, Ryu J (2016) Status and perspectives of multiferroic magnetoelectric composite materials and applications. *Actuators* 5(1). MDPI AG
- [9] Lupascu DC, Wende H, Etier M, Nazrabi A, Anusca I, Trivedi H, Shvartsman VV, Landers J, Salamon S, Schmitz-Antoniak C (2015) Measuring the magnetoelectric effect across scales. *GAMM Mitteilungen* 38(1):25–74
- [10] Naveed-UI-Haq M, Shvartsman VV, Trivedi H, Salamon S, Webers S, Wende H, Hagemann U, Schröder J, Lupascu DC (2018) Strong converse magnetoelectric effect in (Ba, Ca)(Zr, Ti)O<sub>3</sub> - NiFe<sub>2</sub>O<sub>4</sub> multiferroics: a relationship between phase-connectivity and interface coupling. *Acta Mater* 144:305–313
- [11] Naveed-UI-Haq M, Shvartsman VV, Trivedi H, Salamon S, Webers S, Wende H, Hagemann U, Schröder J, Lupascu DC (2020) Corrigendum to ‘Strong converse magnetoelectric effect in (Ba,Ca)(Zr,Ti)O<sub>3</sub>-NiFe<sub>2</sub>O<sub>4</sub> multiferroics: a relationship between phase-connectivity and interface coupling’ *Acta Materialia* 144 (2018) 305–313. *Acta Materialia* 187:91–92. <https://doi.org/10.1016/j.actamat.2017.10.048>

- [12] Kežionis A, Orliukas AF, Paulavicius K, Samulionis V (1991) Methods for determination of electrical and acoustic properties of superionics and mixed ionic-electronic conductors. *Mater Sci Forum* 76:229–232
- [13] Borisov P, Hochstrat A, Shvartsman VV, Kleemann W (2007) Superconducting quantum interference device setup for magnetoelectric measurements. *Rev Sci Instrum* 78(10):106105
- [14] Cordero F, Craciun F, Dinescu M, Scarisoreanu N, Galassi C, Schranz W, Soprunyuk V (2014) Elastic response of  $(1-x)\text{Ba}(\text{Ti}_{0.8}\text{Zr}_{0.2})\text{O}_3-x(\text{Ba}_{0.7}\text{Ca}_{0.3})\text{TiO}_3$  ( $x = 0.45-0.55$ ) and the role of the intermediate orthorhombic phase in enhancing the piezoelectric coupling. *Appl Phys Lett* 105(23)
- [15] Zhang L, Zhang M, Wang L, Zhou C, Zhang Z, Yao Y, Zhang L, Xue D, Lou X, Ren X (2014) Phase transitions and the piezoelectricity around morphotropic phase boundary in  $\text{Ba}(\text{Zr}_{0.2}\text{Ti}_{0.8})\text{O}_3-x(\text{Ba}_{0.7}\text{Ca}_{0.3})\text{TiO}_3$  lead-free solid solution. *Appl Phys Lett* 105(16)
- [16] Damjanovic D, Biancoli A, Batooli L, Vahabzadeh A, Trodahl J (2012) Elastic, dielectric, and piezoelectric anomalies and Raman spectroscopy of  $0.5\text{Ba}(\text{Ti}_{0.8}\text{Zr}_{0.2})\text{O}_3-0.5(\text{Ba}_{0.7}\text{Ca}_{0.3})\text{TiO}_3$ . *Appl Phys Lett* 100(19)
- [17] Galizia P, Baldisserrri C, Mercadelli E, Capiani C, Galassi C, Algueró M (2020) A glance at processing-microstructure-property relationships for magnetoelectric particulate PZT-CFO composites. *Materials (Basel)* 13(11):2592
- [18] Huan Y, Wang X, Fang J, Li L (2014) Grain size effect on piezoelectric and ferroelectric properties of  $\text{BaTiO}_3$  ceramics. *J Eur Ceram Soc* 34(5):1445–1448
- [19] Kambale KR, Mahajan A, Butee SP (2019) Effect of grain size on the properties of ceramics. *Met Powder Rep* 74(3):130–136
- [20] Hao J, Bai W, Li W, Zhai J (2012) Correlation between the microstructure and electrical properties in high-performance  $(\text{Ba}_{0.85}\text{Ca}_{0.15})(\text{Zr}_{0.1}\text{Ti}_{0.9})\text{O}_3$  lead-free piezoelectric ceramics. *J Am Ceram Soc* 95(6):1998–2006
- [21] Carter CB, Norton MG (2013) *Ceramic materials: science and engineering*. Springer, New York
- [22] Lu SG, Xu ZK, Wang YP, Guo SS, Chen H, Li TL, Or SW (2008) Effect of  $\text{CoFe}_2\text{O}_4$  content on the dielectric and magnetoelectric properties in  $\text{Pb}(\text{Zr}, \text{Ti})\text{O}_3/\text{CoFe}_2\text{O}_4$  composite. *J Electroceramics* 21(1–4):398–400
- [23] Yu Z, Ang C (2002) Electrical and magnetic properties of  $\text{BaTiO}_3-(\text{Ni}_{0.3}\text{Zn}_{0.7})\text{Fe}_{2.1}\text{O}_4$  composites. *J Mater Sci Mater Electron* 13(4):193–196
- [24] Bammannavar BK, Naik LR (2009) Electrical properties and magnetoelectric effect in  $(x)\text{Ni}_{0.5}\text{Zn}_{0.5}\text{Fe}_2\text{O}_4+(1-x)\text{BPZT}$  composites. *Smart Mater Struct* 18(8)
- [25] Rehwald W (1973) The study of structural phase transitions by means of ultrasonic experiments. *Adv Phys* 22(6):721–755
- [26] Acosta M, Khakpash N, Someya T, Novak N, Jo W, Nagata H, Rossetti GA, Rödel J (2015) Origin of the large piezoelectric activity in  $(1-x)\text{Ba}(\text{Zr}_{0.2}\text{Ti}_{0.8})\text{O}_3-x(\text{Ba}_{0.7}\text{Ca}_{0.3})\text{TiO}_3$  ceramics. *Phys Rev B Condens Matter Mater Phys* 91(10):1–11
- [27] Cordero F (2018) Elastic and dielectric evaluation of the piezoelectric response of ferroelectrics using unpoled ceramics. *Ceramics* 1(2):211–228
- [28] Acosta M, Novak N, Jo W, Rödel J (2014) Relationship between electromechanical properties and phase diagram in the  $\text{Ba}(\text{Zr}_{0.2}\text{Ti}_{0.8})\text{O}_3-x(\text{Ba}_{0.7}\text{Ca}_{0.3})\text{TiO}_3$  lead-free piezoceramic. *Acta Mater* 80:48–55
- [29] Damjanovic D, Biancoli A, Batooli L, Vahabzadeh A, Trodahl J (2012) Elastic, dielectric, and piezoelectric anomalies and Raman spectroscopy of  $0.5\text{Ba}(\text{Ti}_{0.8}\text{Zr}_{0.2})\text{O}_3-0.5(\text{Ba}_{0.7}\text{Ca}_{0.3})\text{TiO}_3$ . *Appl Phys Lett* 100(19):192907

**Publisher's Note** Springer Nature remains neutral with regard to jurisdictional claims in published maps and institutional affiliations.